Universiteit Leiden
The Netherlands

Activation of G protein-coupled receptors : the role of extracellular loops in adenosine receptors

Peeters, M.C.

Citation
Peeters, M. C. (2011, November 17). *Activation of G protein-coupled receptors : the role of extracellular loops in adenosine receptors*. Retrieved from https://hdl.handle.net/1887/18092

Version:	Corrected Publisher's Version
License:	Licence agreement concerning inclusion of doctoral thesis in the Institutional Repository of the University of Leiden
Downloaded from:	https://hdl.handle.net/1887/18092

Note: To cite this publication please use the final published version (if applicable).

CHAPTER 5

SCREENING FOR CONSTITUTIVELY INACTIVE MUTANTS OF THE ADENOSINE A_{2B} RECEPTOR IN *S. CEREVISIAE*

This chapter was based upon:

M.C. Peeters, Q. Li, G.J.P. van Westen, C.E. Müller, A.P. IJzerman. **2011** (manuscript in preparation)

ABSTRACT

Despite decades of extensive research on G protein-coupled receptors (GPCRs) and the recent elucidation of several high resolution crystal structures, the activation mechanism of these membrane-bound proteins is still largely unknown. Here we describe a new screening method that can greatly aid in the search for specific residues and domains involved in the activation process of GPCRs. By altering the parameters of a random mutagenesis screen using the MMY24 *S. cerevisiae* strain, we successfully screened a region of the human adenosine A_{2B} receptor that includes transmembrane domain 4 (TM4), the second extracellular loop (EL2), and transmembrane domain 5 (TM5), for constitutively inactive mutant receptors (CIMs). The screen resulted in the identification of 22 single and double mutant receptors, all showing a decrease in constitutive activity as well as in agonist potency. A particular important region located at the extracellular half of TM5 was discovered with $C190^{5.46}$ as a key player. This new screening strategy could be applied to all GPCRs that can be functionally expressed in yeast.

INTRODUCTION

G protein-coupled receptors (GPCRs) form one of the largest protein families known and are involved in a wide variety of physiological processes. They constitute the major drug targets of today's medicines, representing approximately 40% of drugs used in the clinic [1] . Therefore, much research is and has been devoted to the elucidation of the function of this large family of membrane proteins, the general structure of which includes seven conserved transmembrane domains connected by intra- and extracellular loops. We now have access to a handful of high resolution crystal structures that allow a hitherto unprecedented three-dimensional view of the receptor [2,3]. However, the currently available structures are only beginning to inform us about the more dynamic process of receptor activation, and, hence, other experimental approaches, such as mutation studies, are still very much needed. GPCRs are supposed to exist in multiple conformations. In a simple scheme an equilibrium exists between an inactive (R) and active conformation (R*) [4]. This assumes a basal activation state of the receptor corresponding to the fraction of R* in the total receptor population. This activation state is essential in maintaining physiological function and many pathogenic mutations have been reported that disturb the equilibrium causing an increase in activation (Constitutively Active Mutants or CAMs) or a decrease in basal activity (Constitutively Inactive Mutants or CIMs) [5,6,7]. These mutations have not only increased our knowledge on the pathophysiology in which GPCRs play a role, but also advanced our insight in the structure-function relationship of GPCRs. Furthermore, CIMs have been found beneficial to stabilize receptors for crystallization purposes, e.g. the β_1-adrenergic receptor [8].

Next to more classical site-directed mutational studies, random mutagenesis approaches have proven to be a very useful tool in identifying residues important for receptor function in an unbiased way [9,10,11]. *S. cerevisiae* is an attractive expression system for subsequent screening since it offers the genetic engineering tools typical of a microorganism while possessing a eukaryotic type of signaling pathway and post-translational modification. During the last decade various GPCRs have been successfully expressed in *S. cerevisiae* [12,13]. Several previous reports

have shown that GPCR function in this eukaryotic system resembles their action in mammalian cell lines [14,15].

The adenosine A_{2B} receptor ($A_{2B}R$) is part of a small subfamily of class A GPCRs, the adenosine receptors. The family consists of four subtypes, the A_1R, $A_{2A}R$, $A_{2B}R$, and A_3R, of which the $A_{2B}R$ has been studied least. Although all adenosine receptors are activated by adenosine, the $A_{2B}R$ has a markedly lower affinity for the endogenous ligand compared with the other three subtypes [16]. Upon metabolic stress, extracellular adenosine is accumulated in the body, activating first the A_1R, $A_{2A}R$ and A_3R subtypes. Only when the adenosine levels rise to high micromolar concentrations, the low affinity $A_{2B}R$ is activated [17]. Activation of the $A_{2B}R$ is essential at this time point in regulating the body's immune response. It is therefore an interesting drug target for several (auto)-immune diseases such as COPD and asthma [18,19,20]. Identifying residues important for activating (or inactivating) the receptor could be of great use in designing drugs for this target.

Here, we describe a new method to screen for constitutively inactive mutants (CIMs) of the adenosine A_{2B} receptor. We created an undirected random mutagenesis library of the $A_{2B}R$ containing mutations in the region encoding transmembrane domain 4 (TM4), the second extracellular loop (EL2), and transmembrane domain 5 (TM5). This library was subsequently screened in a *S. cerevisiae* expression system for a loss-of-function phenotype. This *S. cerevisiae* strain has been genetically modified to serve as a reporter system with growth as an output parameter, and has been used previously as a tool to screen for mutant receptors with *increased* activity compared to wild type receptor [15,21,22]. By adjusting two screening parameters, i.e. the concentration of an inhibitor of histidine synthesis and the selection time, we were able to use the same yeast system to screen for mutant receptors with *decreased* activity. The CIM screening method could be applied to all other GPCRs that can be functionally expressed in yeast. The results obtained for the $A_{2B}R$ proved greatly beneficial in experimentally supporting the structural changes observed between the inactive and active conformations of the closest family member, the $A_{2A}R$, and could provide new insights in the activation mechanism of other class A GPCR family members.

MATERIALS AND METHODS

DNA Constructs

The S*. cerevisiae* expression vector containing the adenosine A_{2B} receptor gene, the pDT-PGK_A_{2B}R plasmid, was kindly provided by Dr. Simon Dowell from GSK (Stevenage, UK). A KpnI restriction site was introduced in the A_{2B}R gene in the region encoding the second intracellular loop, making it possible to divide the receptor into three large fragments suitable for random mutagenesis.

Mutagenic PCR for construction of the random mutagenesis library

Introducing random mutations in the adenosine A_{2B} receptor was achieved by manipulating the polymerase chain reaction adapted from the method of Fromant et al. [23]. The mutagenic PCR reaction was performed in the presence of 10 mM Tris-HCL (pH 9.0), 50 mM KCl, 0.1% Triton X-100, 10 ng of template DNA, 0.1 µM concentrations of each primer, 0.2 mM dATP, 0.2 mM dTTP, 0.2 mM dGTP, 3.4 mM of the nucleotide in excess dCTP, 0.5 mM $MnCl_2$, 4.7 mM $MgCl_2$, and 0.5 units of Super *Taq* polymerase without proofreading (HT Biotechnology LTD, Cambridge, England). The number of mutagenic PCR cycles was set to 10 (PCR cycling conditions: 95ºC for 30 s, 59 ºC for 30 s, 72 ºC for 30s). Using these conditions, only a limited amount of mutations are introduced per fragment [9].

The following primers were used:

5'-GGTATAAAAGTTTGGTCACGGGTACCCGAGCAA-3'

5'-GAAGCTGCCTGCAGGCCACCAGGAAGATCTTAATG-3'

The resulting fragment comprises the region of the adenosine A_{2B} receptor gene that encodes transmembrane domain four (TM4), the second extracellular loop (EL2), and transmembrane domain five (TM5). The mutagenic PCR products were submitted to agarose gel electrophoresis and the gel bands containing the mutated fragments were isolated from the gel and purified. Subsequently, the mutated fragments were amplified further with 10 cycles of a regular PCR with the same primer sets and a polymerase with proofreading, AccuPrime *Pfx* DNA polymerase (Invitrogen, La Jolla, CA, USA) according to the guidelines provided by the manufacturer.

The wild-type fragment TM4-EL2-TM5 in the receptor was subsequently replaced by the mutated fragments using the restriction sites KpnI and BglII, resulting in a mutagenic pDT-PGK- A_{2B}R receptor library.

Transformation in MMY24 S. cerevisiae strain

pDT-PGK_A_{2B}R plasmids were transformed into an *S. cerevisiae* yeast strain according to the Lithium-Acetate procedure [24]. The strain is derived from the MMY11 strain [25] and was further adapted to communicate with mammalian GPCRs through the introduction of a chimeric G protein [13]. The genotype of the MMY24 strain is: *MAT**a**his3 leu2 trp1 ura3can1 gpa1_::G_i3 far1 ::ura3 sst2_::ura3 Fus1::FUS1-HIS3 LEU2::FUS1-lacZ ste2_::G418R.* To measure signaling of GPCRs, the pheromone signaling pathway of this strain was coupled via the FUS1 promotor to HIS3, a gene encoding the key enzyme in histidine production, imidazole glycerol-phosphate dehydrase. The degree of receptor activation was measured by the growth rate of the yeast on histidine-deficient medium.

Screen for inactive mutant receptors

Initially, we plated the transformed MMY24 yeast cells onto Yeast Nitrogen Based (YNB) agar-medium lacking leucine and uracil to select for plasmid-containing transformants. After incubation of 24 hrs, the plates were washed with liquid YNB medium and the transformants were pooled. We then started the actual screen for constitutively inactive mutant receptors by plating the cells onto YNB agar-medium lacking leucine, uracil and histidine (YNB-ULH) but with 1 mM 1,2,4-aminotriazole (3AT, Sigma-Aldrich, Zwijndrecht, The Netherlands) (plating density: ~ 10,000 cells per 100 mm plate). From our previous experience we had learned that a single yeast transformant containing WT receptor needs about 3 days to reach a full colony, while yeast with a constitutively active mutant receptor reached this stage even faster. With this knowledge, we marked the colonies that had already appeared within three days, and ignored them. One day later, after 4 days of screening, the first set of 100 colonies that then appeared was randomly selected. After 6 days of screening, a second set of colonies were selected. Plasmids were isolated from the yeast colonies using the ZymoPrep II Yeast Plasmid Miniprep kit (Zymo Research, Orange, CA, USA) and mutations were identified using double-stranded sequencing (LGTC,

Leiden, The Netherlands). Mutant receptors containing single or double mutations were retransformed into the yeast strain to confirm their inactivated phenotype.

Solid growth assay

To characterize the mutant receptors further, concentration-growth curves were generated in a solid growth assay. In this assay, yeast cells from an overnight culture were diluted to around 400,000 cells/ml (OD_{600} ≈ 0.02), and droplets of 1.5 µl were spotted on selection agar plates, YNB-ULH, containing 7 mM 3AT and a concentration of 5'-N-ethylcarboxamidoadenosine (NECA), a full agonist on the A_{2B} receptor, ranging from 10^{-9} to 10^{-5} M. After incubation at 30°C for 50 h, the plates were scanned and receptor-mediated yeast growth was quantified with Quantity One imaging software from Bio-Rad (Hercules, CA). The amount of yeast growth was calculated as the density of each spot with a correction for local background on the plate. Data were analyzed using nonlinear regression analysis software available in GraphPad Prism 5.0 (GraphPad Software, San Diego, CA).

Liquid growth assay and Schild plot analysis

Similar concentration-growth curves can be produced using liquid selection medium. This assay is in a higher-throughput 96-well format and growth is easily determined by measuring absorption at a wavelength of 595 nm. In this assay, 150 µl liquid YNB-ULH medium with 7 mM 3AT and a varying concentration of ligand was added to each well. Yeast cells from an overnight culture were diluted to around $4 \cdot 10^6$ cells/ml (OD_{600} ≈ 0.2) and 50 µl was added per well. The 96-wells plate was then incubated for 35 hours in a Genios plate reader (Tecan, Durham, NC) at 30°C, keeping the cells in suspension by shaking every 10 minutes at 300 rpm for 1 min. The final absorption values at 595 nm after 35 hours were used as input for the concentration-response curves. Data were analyzed using nonlinear regression analysis software available in GraphPad Prism 5.0 (GraphPad Software, San Diego, CA).

For the wild type A_{2B} receptor and for the mutant receptors $I136L^{4.56}$ and $T162S^{EL2}$/$S180C^{5.36}$, concentration-growth curves of agonist NECA were recorded in the presence of increasing concentrations of the selective A_{2B}R antagonist PSB603 [22, 26]. Schild analysis was performed using the appropriate equations available in GraphPad Prism 5.0.

Whole cell radioligand binding

Yeast cells expressing wild type or mutated $A_{2B}R$ were cultured overnight in rich YAPD (Yeast-extract Adenine Peptone Dextrose) medium. Cells were centrifuged for 5 minutes at 2000 x *g*, and the cell pellet was once washed with 0.9% NaCl. The cells were again centrifuged for 5 min at 2000 x *g* and diluted in the assay buffer (50 mM Tris-HCl pH7.4 + 1 mM EDTA) to OD_{600}=40 (an OD_{600} value of 1 corresponds to approx. $2 \cdot 10^7$ cells/ml). Binding experiments were performed with 1.2 nM [^{3}H]PSB-603 and a final concentration of $25 \cdot 10^7$ cells/ml in a total volume of 100 µl [26]. Nonspecific binding was determined in the presence of 1 mM NECA. Samples were incubated for 1 hour at 25 ºC while shaking vigorously to keep the yeast cells in suspension. Incubation was terminated by adding 1 ml ice-cold assay buffer. Bound from free radioligand was immediately separated by rapid filtration through Whatman GF/B filters pre-incubated with 0.1% polyethylenimine (PEI) using a Millipore manifold during which the filters were washed six times with ice-cold assay buffer. Filter-bound radioactivity was determined by scintillation spectrometry (Tri-Carb 2900TR; PerkinElmer Life and Analytical Sciences) after addition of 3.5 ml of PerkinElmer Emulsifier Safe.

Whole cell extracts and immunoblotting

Whole protein cell extracts were made from the transformed yeast cells using trichloroacetic acid (TCA). From an overnight culture, $1.2 \cdot 10^8$ yeast cells were harvested in mid-log phase. The cells were washed twice with 20% TCA after which they were broken by vigorous vortexing in the presence of glass beads. The yeast cell extracts were separated using SDS/PAGE and subsequently blotted on Hybond-ECL membranes. For this purpose, a sample of 1.0 µl containing 3 µg protein was loaded on a 12.5% SDS/PAGE gel. A semi-automated electrophoresis technique (PhastSystem™, Amersham Pharmacia Biotech) was used for SDS/PAGE as well as blotting. The antibody directed against the C-terminal region of the adenosine A_{2B} receptor was kindly provided by Dr. I. Feoktistov (Vanderbilt University, Nashville). A low range molecular weight standard was used to assess the MW of the bands (Bio-Rad, Hercules, CA). Selective $A_{2B}R$ bands are found at 29 kDa and 48 kDa.

Densitometric analysis of the protein bands was performed using the volume analysis tool as present in the Quantity One imaging software from Bio-Rad (Hercules, CA).

The aspecific band at approximately 45 kDa was used as loading control. The ratio between specific $A_{2B}R$ protein bands and the aspecific band was determined and the wild type receptor was set at 100%, the empty vector pDT-PGK at 0%.

Mapping mutated residues onto the $A_{2A}R$ structure

The positions of the mutations identified in the random mutagenesis screen were mapped onto the corresponding positions in the crystal structure of the adenosine A_{2A} receptor co-crystallized with agonist NECA [27]. These corresponding positions were determined by a multiple sequence alignment created using ClustalW with default parameters. To make use of known crystallographic data, the sequences of the CXCR4 Chemokine (CXCR4) receptor and the β2-adrenergic (b2AR) receptor were also included in this alignment [28,29]. The EL2 was defined from the crystal structures of the A_{2A} receptor (residues 143 to 173), the CXCR4 (residues 175 to 192) and the b2AR (residues 171 to 196).

RESULTS

*General strategy used*We expressed a mutagenized library of the human adenosine A_{2B} receptor in the *Saccharomyces cerevisiae* strain MMY24 [13]. The pheromone signaling pathway of the wild-type MATa mating type yeast uses the Ste2p receptor, a G protein-coupled receptor. Upon activation of this receptor, a mitogen-activated protein kinase cascade is activated through the endogenous Gpa1p G protein, resulting in the transcription of mating genes such as FUS1. The engineered yeast strain MMY24 that we used lacks the endogenous Ste2p receptor, while still maintaining the G protein signaling machinery. To enable G protein coupling to human receptors expressed in this platform, a chimeric Gαi3 protein was introduced of which the last four amino acids of the otherwise yeast G protein were exchanged with the human sequence. Moreover, the HIS3 gene encoding the enzyme imidazole glycerol-phosphate dehydrase (IGPD) that is crucial for the production of the yeast essential amino acid histidine was placed behind the FUS1 promoter [13]. As a result, in the absence of histidine, the only yeast cells able to grow are those in which the expressed GPCR is active (**Figure 1A**).

Even though expression of IGPD is under control of the FUS1 promoter, the yeast strain produces a basal level of histidine without an active receptor present. To suppress the resulting basal growth of the yeast cells, a competitive inhibitor of the enzyme IGPD, 1,2,4-aminotriazole (3AT) is routinely added in order to measure growth that is only caused by an activated receptor. When recording a concentration-growth curve with increasing concentrations of 3AT, we noticed a difference in response between yeast cells that express the human $A_{2B}R$ and those that are only transformed with the empty vector pDT-PGK (**Figure 1B**). At a concentration of 1 mM 3AT, the window between the two curves was most pronounced. At this concentration, yeast cells with an empty vector hardly grew in contrast to yeast cells expressing the $A_{2B}R$. Mutant $A_{2B}Rs$ that display increased activation showed a larger than wild-type response at this 3AT concentration (data not shown). We hypothesized that mutant receptors with decreased activity would 'reside' in between the curves of the wild-type receptor and that of the empty vector. We set out to design a screening method that would select these less active, but still vital mutant receptors.

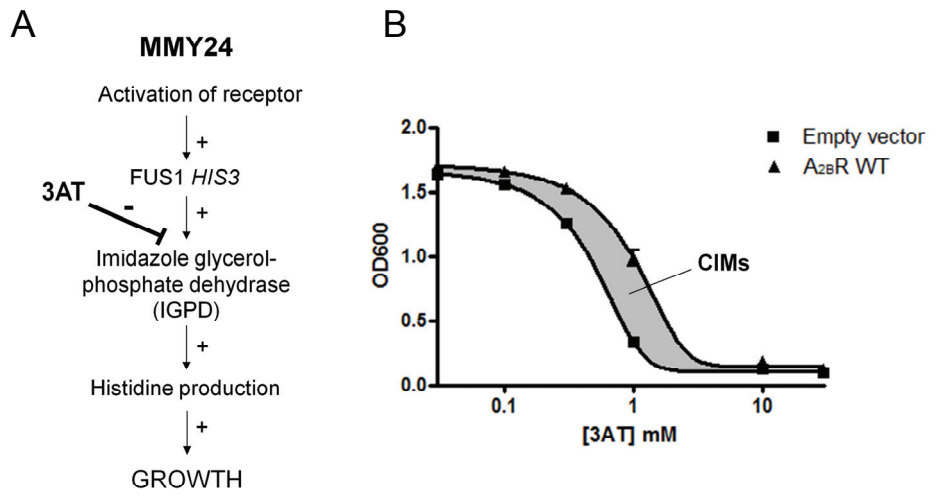

Figure 1. General principle of the yeast genetic screen. *(A)* Schematic representation of the effect of receptor activation in the MMY24 yeast strain. Upon activation, signaling through the G protein pathway leads to transcription of the HIS3 gene. This results in the production of histidine by the cell enabling the yeast cells to grow on histidine-deficient medium. 1,2,4-aminotriazole (3AT) is a competitive inhibitor of the enzyme IGPD, and suppresses growth levels in a dose-response manner. *(B)* Concentration- growth curves with increasing concentrations of 3AT in yeast cells transformed with wild type $A_{2B}R$ or empty vector. The area between the two curves is where receptors with decreased activation profiles can be found.

Random mutagenesis and yeast genetic screen

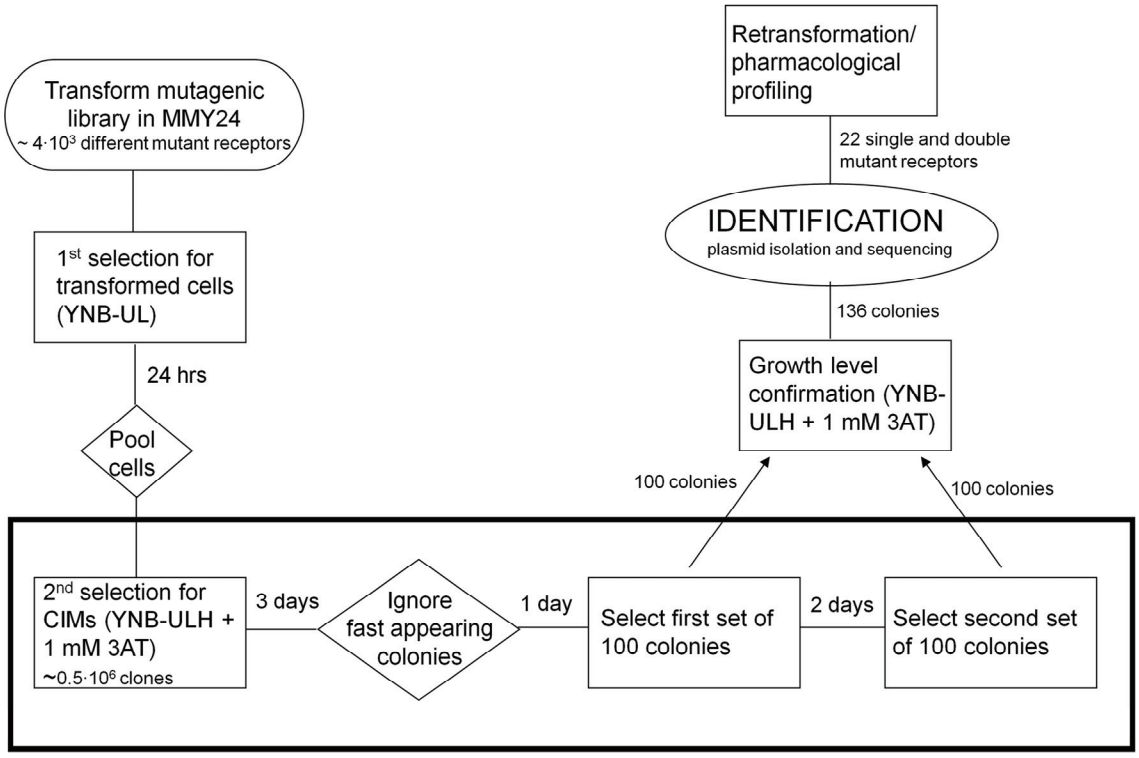

Figure 2. Flow scheme of the screen set-up. After transformation of the library, a first selection is performed for successfully transformed cells. After 24 hrs, cells are pooled and spread onto selection plates without the marker histidine (H) and with a concentration of 1mM 3AT to start the actual screen (indicated in the box). After 3 days, colonies are marked but ignored. The first selection round is one day later, after 4 days. A second selection takes places 2 days after the first, in total after 6 days. All colonies were checked independently in comparison with wild type receptor on new selection plates. From the positive clones, plasmid was isolated, sequenced, and retransformed to characterize the identified mutant receptors.

The protocol we followed is depicted as a flow scheme in **Figure 2**. A silent mutation was introduced in the second intracellular loop of the $A_{2B}R$ gene in order to insert a KpnI restriction site. Using this and the BglII restriction site, the receptor gene was divided into three parts that each has a suitable length for random mutagenesis purposes. For the random mutagenesis experiments in the present study a fragment of 262 base pairs encoding transmembrane domain 4 (TM4), the second extracellular loop (EL2) and transmembrane domain 5 (TM5) was used. Mutations were randomly introduced using a mutagenic PCR where an excess of the nucleotide dCTP was added. The PCR conditions were optimized to generate a large number of mutated receptors with a relatively low mutation frequency. After mutagenesis, the normal fragment TM4-EL2-TM5 in the wild type receptor was replaced by the mutated

fragments using the restriction sites KpnI and BglII, resulting in a mutagenic adenosine A_{2B} receptor library containing approximately 4000 different mutant receptors, ranging from a one-nucleotide change to a maximum of five mutations per fragment. The mutagenized A_{2B}R library was expressed in the MMY24 yeast strain and screened for an inactivating phenotype using selection plates lacking histidine and with 1 mM 3AT as discussed before (**Figure 2**). At this concentration yeast expressing the wild type A_{2B}R was still able to grow, but cells containing the empty vector did so only marginally, if at all. To eliminate yeast cells from the screening library that did not contain a plasmid, we first pre-screened for successfully transformed yeast cells. In total, ca. 0.5 million yeast clones were used for the final inactivation screen, so the library was screened approximately 100 times. To avoid selecting mutant receptors with increased levels of activity, we also introduced a time restraint. The more active a receptor, the more histidine the yeast cell produces. This results in more, but also faster growth of the cells. In our hands a yeast cell expressing wild type A_{2B}R typically needs 72 hrs to form a reasonably sized colony, while yeast with more active receptors reach this stage sooner. By applying this time frame as a threshold, we ignored receptors with increased activation and only focused on the less active mutants. We used two time points at which we selected colonies, after 4 days and again after 6 days of screening. At each of these two time points we randomly picked 100 colonies. All 200 colonies were subjected to a second selection procedure to confirm their growth levels. True hits were considered colonies that were able to grow on selection plates containing 1 mM 3AT, but less than the wild type receptor (the green bars in **Figure 3**). Other colonies not meeting our criteria, were not sequenced (the red bars in **Figure 3**). Approximately 70% of the selected colonies met these criteria, yielding 136 colonies of interest. The high hit rate indicates that the parameters used in the previous screen were successful.

Plasmids were isolated from ‘hit’ colonies and mutations were identified by sequence analysis. Among the plasmids isolated from the first selection at day 4, only a few wild type receptors were still present. Most mutant receptors contained one or two amino acid changes. Plasmids isolated from the second selection at day 6 contained no wild type receptors anymore. The identified mutant receptors at this stage showed larger defects with more multiple amino acid changes, and also deletion mutants were found. This selection also contained expected “receptor killers”, like a mutation

of the cysteine at position 171^{EL2}. This cysteine is part of the conserved disulfide bridge formed with a cysteine in TM3 that is present in over 90% of all class A GPCRs and is considered essential in receptor structure and function. Mutant receptors containing only one or two amino acid changes, in total 22 mutants, were chosen for further characterization and were retransformed into the yeast strain to confirm their inactive phenotype.

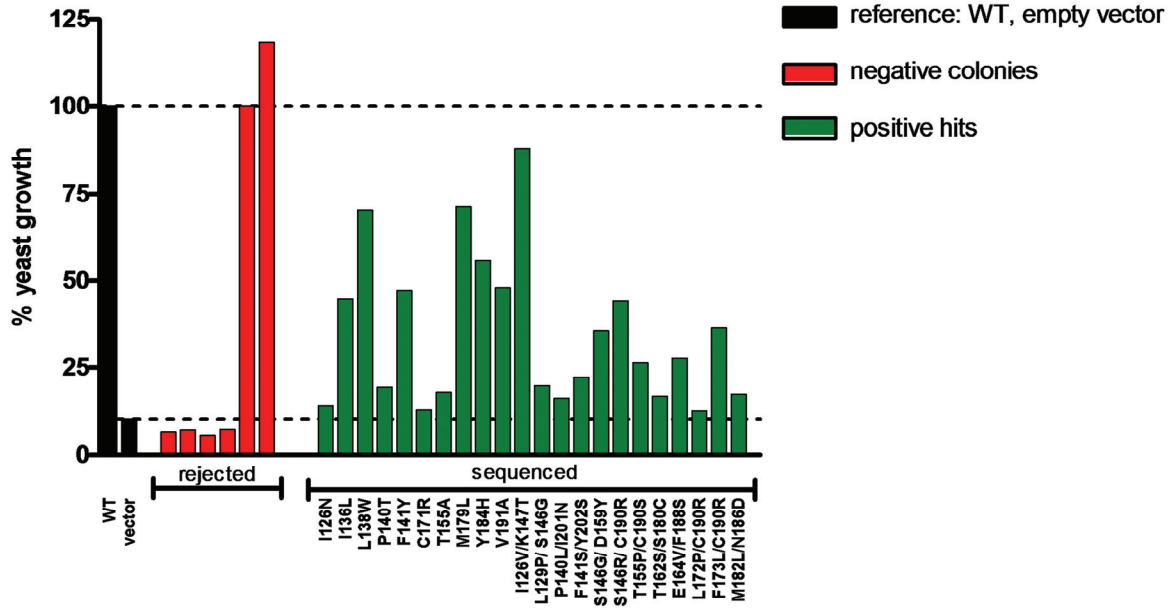

Figure 3. Results from reconfirmation screen. A total of 200 colonies selected from the CIM screen were subjected again to selection plates containing 1 mM 3AT. Positive hits were clones that showed growth levels lower than wild type, but higher than the empty vector (green). Receptor mutations from these colonies were identified by sequencing. Colonies that grew less than the empty vector or more than wild type were rejected (red). A selection of mutant receptors is shown in the graph, where growth of wild type (WT) is set to 100%, 0% was set to the background of the selection plate.

Characterization of mutant adenosine A_{2B} receptors

We mapped the mutated residues found in the single and double mutants onto the snake-plot of the A_{2B}R sequence in red (**Figure 4**). The residues are present all over the mutated fragment (indicated in the figure as between the restriction sites KpnI and BglII), with a large number of mutated residues located at the top half of TM5. The isolated plasmids containing one or two amino acid changes were retransformed into the MMY24 yeast strain and full concentration-growth curves were recorded to investigate their pharmacologic profile.

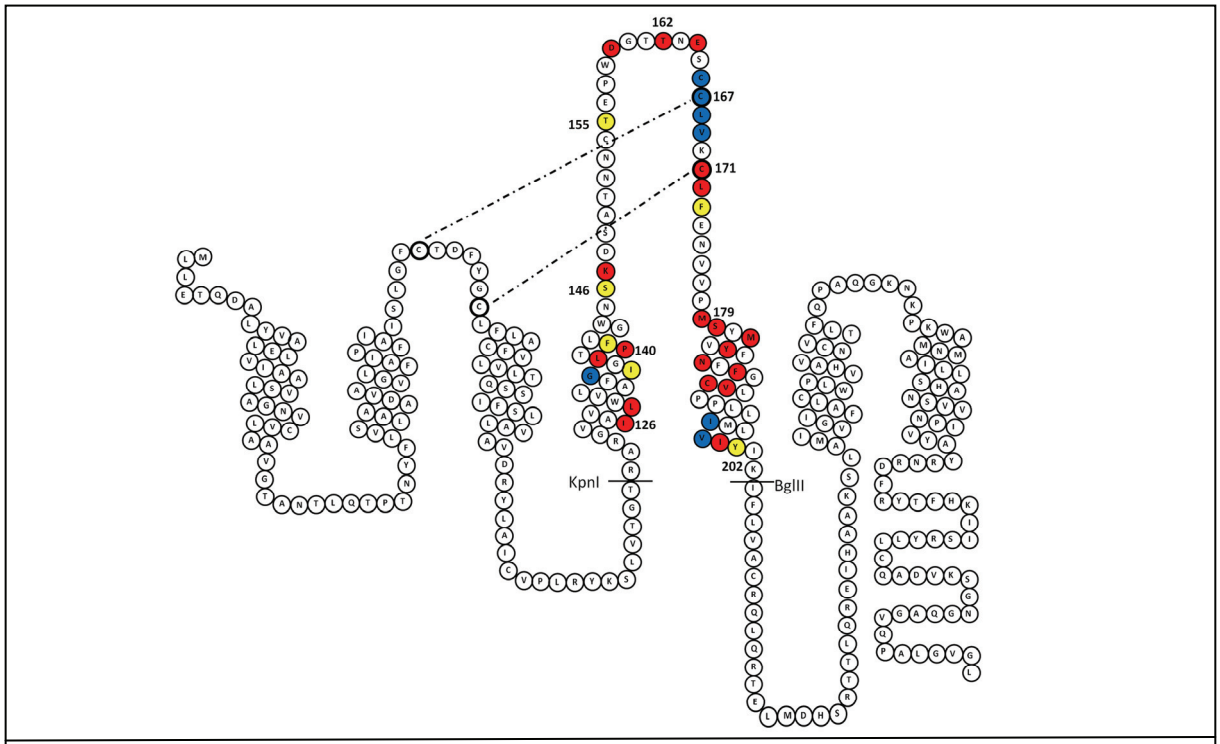

Figure 4. Snake-like representation of the adenosine A_{2B} receptor sequence showing both CIM and CAM residues identified in our screens. Residues found mutated as single and double mutant receptors in the CIM screen are shown in red. The CAM residues identified in a previous screen are shown in blue. Overlapping residues are shown in yellow. The putative disulfide bridges are indicated with dotted lines. The disulfide bridge conserved in many class A GPCRs links C78 and C171. The non-conserved second disulfide bridge between EL1 and EL2 based on the crystal structures of the adenosine $A_{2A}R$, links C72 and C167. The restriction sites KpnI and BglII are indicated that were used to obtain the fragment for random mutagenesis.

All of the 22 mutant receptors tested showed a decrease in potency vs wild-type in response to the full agonist NECA (see **Figure 5** for five representative mutants), ranging from a slight decrease in potency ($T162S^{EL2}$/$S180C^{5.36}$) to a full loss of activation ($C171R^{EL2}$). Only three mutant receptors ($I136L^{4.56}$, $T155A^{EL2}$, $T162S^{EL2}$/$S180C^{5.36}$) were still able to reach near-maximal activation levels. A full list of all the tested mutant receptors and their response to NECA is in **Table 1**.

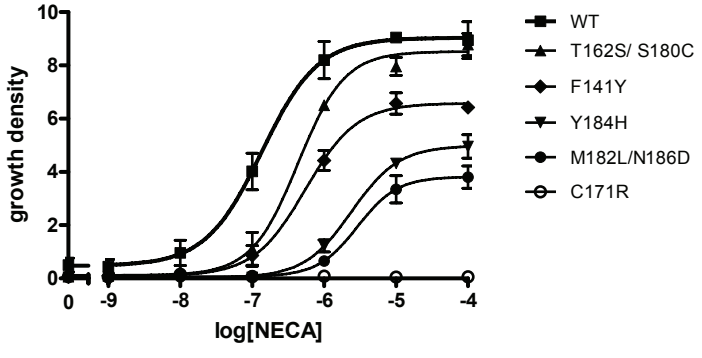

Figure 5.
Representative concentration-growth curves of mutant receptors. Yeast growth was measured on selective agar plates YNB-ULH with increasing NECA concentrations. Mutant receptors T162S/S180C (▲), F141Y (♦), Y184H (▼), M182L/N186D (●), and C171R (○), show a representative variety of concentration-growth curves of the mutant receptors identified from the screen. As a reference, the concentration-growth curve of the wild type human $A_{2B}R$ (■) is shown.

Table 1. Characterization of the adenosine receptor A_{2B} receptor mutants with one or two amino acid changes identified from the random mutagenesis screen. EC_{50} values (μM) in response to NECA are shown as means ± SEM of at least three independent experiments, each performed in duplicate. The mean values derived from the concentration-growth curves were used for calculation of the percentage maximal activity (Emax) and the level of constitutive activity (Fold CA), compared to the wild type receptor

Mutant	Fold CA	EC_{50} (μM) NECA	% Emax
WT	1.0	0.14 +/- 0.03	100
$I126N^{4.46}$	0.1	-	-
$I136L^{4.56}$	0.03	1.6 +/- 0.4	101
$L138W^{4.58}$	0.1	-	-
$P140T^{4.60}$	0.1	6.1 +/- 1.0	63
$F141Y^{4.61}$	0.2	0.55 +/- 0.1	73
$T155A^{EL2}$	0.4	1.1 +/- 0.1	102
$C171R^{EL2}$	0.04	-	-
$M179L^{5.35}$	0.1	4.2 +/- 1.1	70
$Y184H^{5.40}$	0.1	2.8 +/- 0.5	55
$V191A^{5.47}$	0.3	14.0 +/- 1.3	53
$I126V^{4.46}$/$K147T^{EL2}$	0.001	1.1 +/- 0.3	60
$L129P^{4.49}$/$S146G^{EL2}$	0.2	-	-
$P140L^{4.60}$/$I201N^{5.57}$	0.2	-	-
$F141S^{4.61}$/$Y202S^{5.58}$	0.1	-	-
$S146G^{EL2}$/$D159Y^{EL2}$	0.1	0.4 +/- 0.05	71
$S146R^{EL2}$/$C190R^{5.46}$	0.1	-	-
$T155P^{EL2}$/$C190S^{5.46}$	0.1	0.7 +/- 0.1	70
$T162S^{EL2}$/$S180C^{5.36}$	0.3	0.4 +/- 0.1	96
$E164V^{EL2}$/$F188S^{5.44}$	0.3	-	-
$L172P^{EL2}$/$C190R^{5.46}$	0.01	-	-
$F173L^{EL2}$/$C190R^{5.46}$	0.1	-	-
$M182L^{5.38}$/$N186D^{5.42}$	0.1	3.5 +/- 0.4	42

Western blot analysis showed that all mutant receptors are being expressed in the yeast cells, most of which in comparable amounts to wild type. Expression levels range from ca. 60% (S146G^{EL2}/D159Y^{EL2}) to ca. 135% (L138W$^{4.58}$). Two representative western blots are shown in **Figure 6**.

Figure 6. Western Blot of several mutant A_{2B} receptors with different activation profiles. Cell lysates of yeast cells transformed with wild type receptor, empty vector pDT-PGK, and mutant receptors were separated by SDS/PAGE and blotted on Hybond-ECL membranes. The arrows indicate the specific bands belonging to the adenosine A_{2B}R; these are located at ca. 29 kDa and 48 kDa.

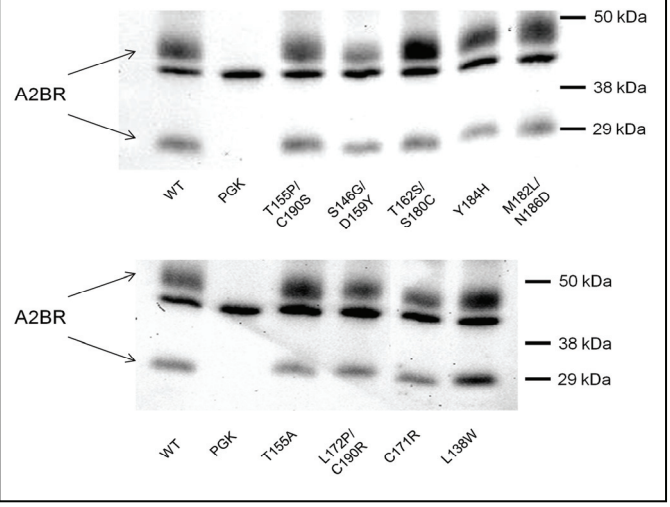

Next, we performed single point radioligand binding experiments using the A_{2B}R selective radiolabeled antagonist [^{3}H]PSB-603 [22,26] and the full agonist NECA (1 mM) as the displacing unlabeled ligand to define non-specific binding. Only three mutant receptors were able to reach levels of binding similar to the wild type receptor (**Figure 7**). All other mutant receptors had decreased levels of binding or were not able to bind the radiolabeled antagonist at all. To investigate whether this loss of radioligand binding was due to a decrease in antagonist affinity next to agonist potency, we performed a Schild plot analysis. Mutant receptors I136L$^{4.56}$ and T162S^{EL2}/S180C$^{5.36}$ were subjected to an increasing concentration of the antagonist PSB-603 in the presence of a concentration range of the agonist NECA and concentration-growth curves were measured (**Figure 8**). Both mutants showed an increase in NECA's EC_{50} value, but were still able to reach maximal growth levels compared to wild type receptor. In the single point radioligand binding assay, mutant I136L$^{4.56}$ bound the radiolabeled antagonist as avidly as wild type receptor, however, mutant T162S^{EL2}/S180C$^{5.36}$ showed a large decrease in radiolabeled antagonist binding. The pA_2 values measured from the Schild plot were 9.2 for wild type, 9.0 for mutant I136L$^{4.56}$, and 8.4 for mutant T162S^{EL2}/S180C$^{5.36}$, indicating that antagonist

affinity for the latter mutant was indeed compromised by the mutation, explaining the lack of radioligand binding (**Figure 8)**.

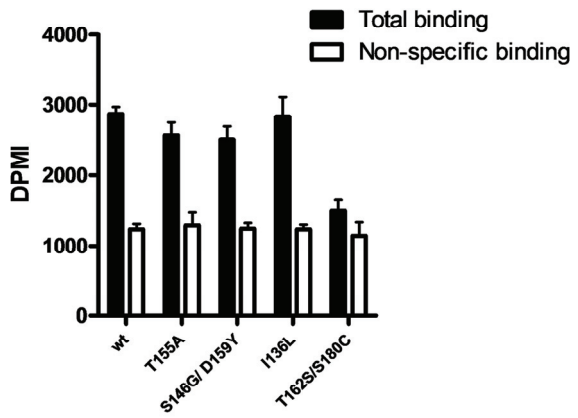

Figure 7. Single point competition binding assay with [^{3}H]PSB603. Binding experiments were performed at a radioligand concentration of 1.2 nM. Non-specific binding was determined using 1 mM NECA, shown in white bars. Total binding is shown in black bars. The mutant receptors shown were able to bind [^{3}H]PSB603 similar to wild type receptor at this concentration. Mutant T162S/S180C is one mutant receptor representative of many mutants with a large decrease in total binding.

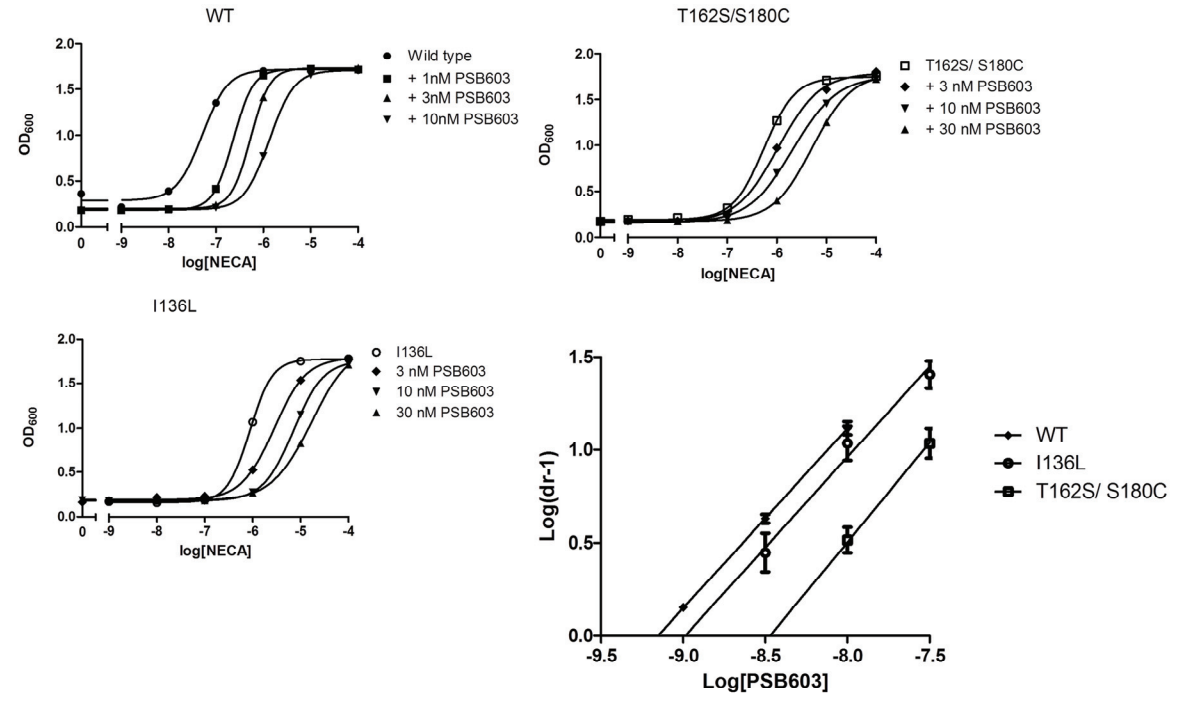

Figure 8. Schild plot analysis of PSB603 binding to WT and mutant receptors T162S/S180C and I136L. *(A)* Concentration-growth curves of NECA were recorded in the absence and presence of three concentrations of antagonist PSB603. *(B)* The pA_2 values of PSB603 were determined from a Schild plot (WT: 9.2, I136L: 9.0, T162S/S180C: 8.4).

Mapping mutated residues onto the $A_{2A}R$ structure

The adenosine A_{2A} receptor, the structure of which was recently elucidated [30], is the closest homologue to the adenosine A_{2B} receptor, with 82 % amino acid similarity and 59 % identity [22]. Therefore, the structure of the A_{2A} receptor could be predictive

of the spatial orientation of the $A_{2B}R$ amino acid residues. To determine which positions in the $A_{2A}R$ correspond to the $A_{2B}R$ CIMs, we created a multiple sequence alignment using all four subtypes of adenosine receptors as well as two other crystallized GPCRs, the β_2-adrenergic receptor [29] and the CXCR4 chemokine receptor [28] (**Figure 9A)**. Since the EL2 of the $A_{2B}R$ is longer than that of the $A_{2A}R$, two residues important for receptor inactivation could not be mapped onto the structure, namely adjacent $S146^{EL2}$ and $K147^{EL2}$. When aligning EL2 of the $A_{2A}R$ with the $A_{2B}R$, the equivalent positions of these two $A_{2B}R$ residues are located in a gap in the alignment (**Figure 9A**). The 3D representation in **Figure 9B**, like **Figure 4**, shows that most mutated residues are found near or in the extracellular region of the receptor; in the top half of TM4, in EL2, and in the top half of TM5. The mutated cluster in EL2 is located in a flexible part of the loop, upstream of the β-strand and in the helical structure as present in the NECA-bound $A_{2A}R$ structure (**Figure 9B**).

DISCUSSION

We set out to develop a new screening method for fast identification of inactivating mutations in the adenosine A_{2B} receptor. In the past, CAMs have provided great insight in how GPCRs can adapt an active conformation, similar to what occurs when an agonist is present [5,21,31]. CIMs represent an inactive state of the receptor, mimicking more the presence of an inverse agonist. By increasing our knowledge on this lesser explored spectrum of the activation mechanism, we aim to provide an enhanced insight of what occurs during receptor activation.

Li and coworkers reported on a different yeast system in which it is possible to screen for inactivating mutations [32]. Their system is highly engineered to only enable yeast cells containing inactive mutant receptors to survive by the introduction of the CAN1 reporter gene. When the receptor is activated, it promotes the expression of a transporter protein for the cytotoxic agent canavanine that leads to cell death. The use of this elegant system proved very successful in screening for residues that are functionally important in the M_3 muscarinic acetylcholine receptor (M_3R) [32,33]. The screening method described here is different in that it does not need a separately constructed system to screen for inactivating or activating mutant receptors. By

simply changing the concentration of the histidine synthesis inhibitor 3AT and the introduction of a specific time frame, we used one and the same system to also screen for inactivating mutant receptors. Also, our screen set-up does not require the presence of an agonist when selecting inactivating mutant receptors. This is beneficial, since then not only mutations that affect the binding and activation mode of that specific agonist are favoured. After identification of the mutant receptors, it is possible to verify their phenotype and investigate their pharmacologic profile again in the same system, without the need of more time-consuming procedures like expressing the mutant receptors in a mammalian cell system. This makes the initial selection of residues of interest faster and more convenient.

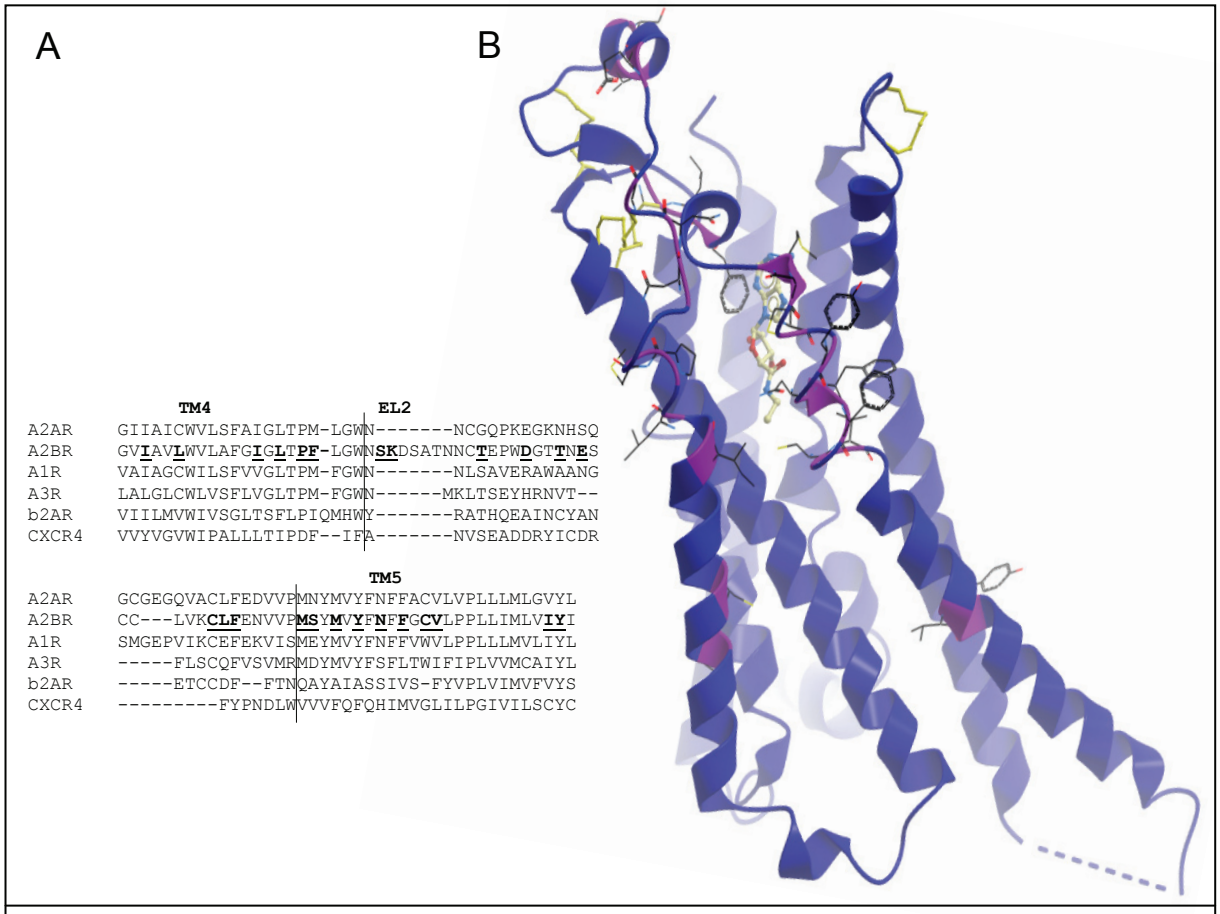

Figure 9. Mutated residues of the $A_{2B}R$ mapped on the crystal structure of the $A_{2A}R$ co-crystallized with NECA. *(A)* The multiple sequence alignment of the $A_{2A}R$ and $A_{2B}R$. The whole alignment was constructed using all four adenosine receptor subtypes as well as the sequence of two other crystal structures (of CXCR4 and β_2-adrenergic receptor) to ensure correct determination of EL2. The transitions between TM domains and EL2 are indicated with vertical lines, the mutated residues are indicated in bold font and underlined. *(B)* Based on the multiple sequence alignment described in Materials and Methods, the mutated residues identified from the screen were mapped onto the crystal structure of the $A_{2A}R$ (PDB: 3YDV) (blue), the closest homologue of the $A_{2B}R$. The mutated residues with their side chains are indicated in magenta. The ribbon representation also shows the co-crystallized ligand NECA (atoms colored) as well the disulfide bridges (yellow) that restrict EL2.

The CIM screen

We started with a random mutagenesis library in which in low frequency mutations were introduced in the fragment TM4-EL2-TM5 of the $A_{2B}R$. We subsequently transformed this library in the MMY24 yeast strain and started to screen at a concentration of 1 mM 3AT, a concentration at which, as a negative control, yeast containing only the expression vector was not able to produce enough histidine to allow substantial growth. However, yeast expressing the wild type $A_{2B}R$ was able to grow at this concentration of 3AT, reaching 50% of the maximal growth level at even lower concentrations of 3AT (**Figure 1**). We selected yeast colonies at two time points in the screen, after 4 days and after 6 days of screening. All selected colonies were first subjected to a reconfirmation procedure, where we looked at relative growth compared to wild type $A_{2B}R$ and a negative control in which only the expression vector was transformed (**Figures 2 and 3**). Out of the 200 colonies tested in this second round 136 colonies showed the correct phenotype (61 originating from day 4 and 75 from day 6 of the selection), indicating that the screen with the chosen parameters was successful (**Figure 3**). Among the colonies that failed this reconfirmation round, only a few showed a higher growth level than wild type (all present in first selection round at day 4). Most colonies that were discarded showed even less growth than the negative control and therefore most likely did not contain a functional receptor. Sequencing of the hits showed that after 4 days of screening the most relevant results were obtained. Mutant receptors showed many single and double amino acid changes, and only a low amount of wild type receptors was found in this selection. After 6 days however, more defects were found, including frame-shifts, deletions and expected “receptor killers”, such as mutation of the conserved cysteine at position 171^{EL2} in EL2.

Characterizing the mutant A_{2B} receptors

All receptors with one or two amino acid changes, in total 22 different mutant receptors, were used for further characterization. All of these single and double mutants showed a decrease in activation profile compared to the wild type receptor. Some were still able to reach full activation levels, others could not be activated by the agonist at all (**Figure 5, Table 1**). Even though several mutant receptors showed no activation whatsoever, they could all be expressed in the yeast system at levels

quite comparable to the wild-type receptor. A representative selection of these is shown in the Western Blot experiment in **Figure 6**. We were also able to measure specific radioligand binding to the A_{2B} wild-type receptor in yeast – in fact one of the few observations of radioligand binding to GPCRs expressed in yeast cells. For that, we used the recently described high-affinity antagonist [^{3}H]PSB-603 [26]. We also demonstrated specific binding to some mutant receptors, while most receptors did not display any binding (**Figure 7**). The Schild plot analysis for double mutant $162S^{EL2}$/$S180C^{5.36}$ in **Figure 8** suggests that this lack of radioliogand binding may be correlated with a decrease in antagonist affinity as determined in the functional growth assay.

In **Figure 9B**, we mapped the mutated residues onto the NECA-bound crystal structure of the adenosine A_{2A} receptor (PDB entry code: 3YDV), showing the putative 3D positions of the three mutated clusters [27]. Random mutagenesis studies of another GPCR expressed in yeast, the complement factor 5a receptor (C5aR), also revealed amino acid clusters important for receptor activation at the extracellular membrane interface that included TM4 and TM5 [34,35]. However, only two residues in the C5aR are located at positions corresponding to mutations found in the screen described here, namely at position 4.58 and 5.42 (L138 and N186 in the A_{2B}R).

The mutations present in TM4 are all pointing to the helical bundle. Presumably, disturbance of these inter-helix interactions may indeed interfere with the activation mechanism of the receptor. TM4 has not been found to play a role in coordinating receptor ligands through direct interactions in any of the available crystal structures. However, it is involved in Van der Waals interactions with TM5, as seen in the inactive crystal structures of the β_1-adreneric receptor and the adenosine A_{2A} receptor. These interactions are disturbed or changed in the activated structure [27,30,36].

In EL2, most residues that upon mutation cause the receptor to lose its ability to be fully activated are located in the more flexible, less restricted regions of the loop. It seems that despite the restrictions imposed by disulfide bridges, the second extracellular loop needs a certain amount of conformational flexibility for efficient receptor activation as has been suggested previously [33,37,38]. The conserved cysteine (C171) in EL2 was found affected too. The disulfide bridge in which it

participates has been reported as essential for maintaining GPCR structure and function [39]. Also F173^{EL2} was found mutated in one of the receptors in our mutant library. A phenylalanine at the corresponding position in the $A_{2A}R$ interacts directly with the bound ligand in all four available crystal structures (**Figure 9B** shows the NECA-bound structure PDB:3YDV) [27,30,40].

In TM5, the mutations are mainly located at the centre of the α-helix. In the active crystal structures of the adenosine $A_{2A}R$, only two residues in TM5 directly contribute to the ligand binding site of NECA and adenosine, namely M177$^{5.38}$ and N181$^{5.43}$ [27]. In our CIM screen, we identified a double mutant in which the two corresponding residues in the A_{2B} receptor were mutated; M182L$^{5.38}$/N186D$^{5.42}$. This mutant receptor had a 25-fold decrease in potency for NECA and was only able to reach 42% of the maximal activation level. Also, no antagonist binding could be observed in the radioligand binding experiments. The other identified residues are not in close proximity (within 5 Å) of the $A_{2A}R$ ligand binding pocket, although they have a strong impact on receptor activation and so form a good starting point in unravelling the activation mechanism and conformational changes of the adenosine A_{2B} receptor.

A number of amino acid positions are found several times in different mutant receptors, like I126$^{4.46}$, P140$^{4.60}$ and F141$^{4.61}$ in TM4, S146^{EL2} and T155^{EL2} in EL2, and C190$^{5.46}$ in TM5. These positions are found mutated into different residues, but also in different combinations with other mutated residues, indicating an especially important role in receptor activation. Residue C190$^{5.46}$ was identified in four different mutant receptors, either mutated to a serine or arginine (S146R^{EL2}/C190R$^{5.46}$, T155P^{EL2}/C190S$^{5.46}$, L172P^{EL2}/C190R$^{5.46}$, F173L^{EL2}/C190R$^{5.46}$), all in combination with a mutation located in EL2. Only mutant receptor T155P^{EL2}/C190S$^{5.46}$ was still able to show an agonistic response to NECA, although potency was reduced 5-fold and the maximal activation level could not be reached (**Table 1**). The corresponding position C185$^{5.46}$ in the $A_{2A}R$ appears to be responsible for a bulge in TM5 that occurs after activation. When comparing the inactive structure (PDB:3EML) bound to ZM241385 with the active structures (PDB: 3QAK/3YDO/3YDV) bound to UK-432097, NECA and adenosine, respectively, TM5 moves slightly inwards, towards TM6. A movement of C185$^{5.46}$ initiates a sequence of changes via V186$^{5.47}$ and H250$^{6.52}$, hereby tightening the ligand binding pocket [27,40]. In the inactive $A_{2A}R$ structure, a Van der Waals interaction exists between C185$^{5.46}$ and I135$^{4.56}$, similar to

the interaction observed in the β_1-adrenergic receptor [8,30]. The corresponding residue in TM4 in the $A_{2B}R$, $I136^{4.56}$, was also identified as a single mutant in our CIM screen. This $I136L^{4.56}$ mutant showed a large decrease in constitutive activity as well as an 11-fold decrease in NECA potency. In the inactive conformation of the $A_{2A}R$, the backbone of $C185^{5.46}$ is also connected by a hydrogen bond to residue $Q89^{3.37}$in TM3. In the active structures, this hydrogen bond cannot be formed anymore. It needs to be noted though that in the NECA and adenosine bound structures, residue $Q89^{3.37}$ has been mutated to an alanine to increase the thermostability of the receptor for crystallization purposes.

Residue $C190^{5.46}$ identified in our screen, is located at the bottom of the cluster in TM5. The other residues present in the cluster might be essential in facilitating the movement of the intracellular half of TM5 and participate in the ligand binding pocket (such as residues $M182^{5.38}$ and $N186^{5.42}$).

Constitutively active mutants (CAMs) versus constitutively inactive mutants (CIMs)

The same mutagenic library as employed in the study described here was previously used by us to screen for constitutively active mutant (CAM) receptors [21]. We used the same MMY24 yeast screen and the same technical approach, with the exception that the screen was performed in the presence of 7 mM 3AT and that colonies were selected after three days instead of the delayed approach described for the CIM screen. From the CAM screen, 12 different mutant receptors were identified that besides increased constitutive activity also displayed an increase in potency for the agonist NECA. The CAMs appeared to form three small clusters; at the top of TM4, in a cysteine-rich region in EL2, and at the bottom of TM5. In **Figure 4**, the identified residues are indicated from both the CIM (in red) and the CAM (in blue) screens. The yellow residues indicate positions that were found mutated in both screens. The previously described CAM clusters in TM4 and TM5 are now also sites for constitutively inactivating mutations. The CAM cluster in EL2, however, remains intact and is therefore likely important in silencing the receptor in its basal state. At the extracellular half of TM5, only CIMs were identified, indicating that this region has an opposite function.

Concluding remarks

By applying our new screening method, we were able to identify residues that are involved in maintaining the equilibrium between the inactive (R) and active (R*) receptor conformation in the absence of a ligand. This yeast screening strategy allowed for a rapid identification of functionally important residues in a typical class A GPCR, the adenosine A_{2B} receptor. This approach may be well applicable to other GPCRs that can be functionally expressed in yeast. Also, the CIMs identified from the newly developed screen, provide detailed insights in the activation mechanism of the A_{2B}R and revealed a particular important role for the upper half of TM5 in facilitating the conformational changes in the process of receptor activation. When these residues are mutated, receptor activity is compromised, either by directly changing the ligand binding site or by influencing conformational changes at a more distant location. The results obtained from this study can help clarify the changes observed between different structural conformations of the crystal structures available and provide mechanistic insight in the activation mechanism of class A GPCRs.

ACKNOWLEDGEMENTS

This research was performed under the auspices of the GPCR Forum, a program funded by the Dutch Top Institute Pharma (project D1-105).

REFERENCES

[1] Kristiansen, K., *Pharmacol Ther* (2004) 103:21-80.
[2] Deupi, X., Standfuss, J., *Curr Opin Struct Biol* (2011) doi 10.1016/j.sbi.2011.06.002.
[3] Peeters, M.C., van Westen, G.J., Li, Q., IJzerman, A.P., *Trends Pharmacol Sci* (2011) 32:35-42.
[4] Leff, P., *Trends Pharmacol Sci* (1995) 16:89-97.
[5] Cotecchia, S., Fanelli, F., Costa, T., *Assay Drug Dev Technol.* (2003) 1:311-316.
[6] Tao, Y.X., *Pharmacol Ther* (2006) 111:949-973.
[7] Kleinau, G., Jaeschke, H., Mueller, S., Worth, C.L., Paschke, R., Krause, G., *Cell Mol Life Sci* (2008) 65:3664-3676.
[8] Warne, T., Serrano-Vega, M.J., Baker, J.G., Moukhametzianov, R., Edwards, P.C., Henderson, R., Leslie, A.G., Tate, C.G., Schertler, G.F., *Nature* (2008) 454:486-491.
[9] Beukers, M., IJzerman, A., *Trends Pharmacol Sci.* (2005) 26:533-539.
[10] Decaillot, F., Befort, K., Filliol, D., Yue, S., Walker, P., Kieffer, B., *Nat Struct Biol.* (2003) 10:629-636.
[11] Hagemann, I., Narzinski, K., Floyd, D., Baranski, T., *J Biol Chem.* (2006) 281:36783-36792.
[12] Minic, J., Sautel, M., Salesse, R., Pajot-Augy, E., *Curr Med Chem* (2005) 12:961-969.

[13] Brown, A., et al., *Yeast* (2000) 16:11-22.
[14] Stewart, G.D., Valant, C., Dowell, S.J., Mijaljica, D., Devenish, R.J., Scammells, P.J., Sexton, P.M., Christopoulos, A., *J Pharmacol Exp Ther* (2009) 331:277-286.
[15] Beukers, M., van Oppenraaij, J., van der Hoorn, P., Blad, C., den Dulk, H., Brouwer, J., IJzerman, A., *Mol Pharmacol.* (2004) 65:702-710.
[16] Fredholm, B.B., IJzerman, A.P., Jacobson, K.A., Linden, J., Muller, C.E., *Pharmacol Rev* (2011) 63:1-34.
[17] Fredholm, B.B., *Cell Death Differ* (2007) 14:1315-1323.
[18] Wilson, C.N., *Br J Pharmacol* (2008) 155:475-486.
[19] Spicuzza, L., Di Maria, G., Polosa, R., *Eur J Pharmacol* (2006) 533:77-88.
[20] Hasko, G., Linden, J., Cronstein, B., Pacher, P., *Nat Rev Drug Discov* (2008) 7:759-770.
[21] Peeters, M.C., Li, Q., Van Westen, G.J., IJzerman, A.P., *Purinergic Signal* (2011) In press.
[22] Peeters, M.C., van Westen, G.J., Guo, D., Wisse, L.E., Muller, C.E., Beukers, M.W., IJzerman, A.P., *FASEB J* (2011) 25:632-643.
[23] Fromant, M., Blanquet, S., Plateau, P., *Anal Biochem* (1995) 224:347-353.
[24] Gietz, D., St Jean, A., Woods, R.A., Schiestl, R.H., *Nucleic Acids Res* (1992) 20:1425.
[25] Olesnicky, N.S., Brown, A.J., Dowell, S.J., Casselton, L.A., *Embo J* (1999) 18:2756-2763.
[26] Borrmann, T., Hinz, S., Bertarelli, D.C., Li, W., Florin, N.C., Scheiff, A.B., Muller, C.E., *J Med Chem* (2009) 52:3994-4006.
[27] Lebon, G., Warne, T., Edwards, P.C., Bennett, K., Langmead, C.J., Leslie, A.G., Tate, C.G., *Nature* (2011) 474:521-525.
[28] Wu, B., et al., *Science* (2010) 330:1066-1071.
[29] Rosenbaum, D.M., et al., *Science* (2007) 318:1266-1273.
[30] Jaakola, V.P., Griffith, M.T., Hanson, M.A., Cherezov, V., Chien, E.Y., Lane, J.R., IJzerman, A.P., Stevens, R.C., *Science* (2008) 322:1211-1217.
[31] Kobilka, B.K., Deupi, X., *Trends Pharmacol Sci* (2007) 28:397-406.
[32] Li, B., Scarselli, M., Knudsen, C., Kim, S., Jacobson, K., McMillin, S., Wess, J., *Nat Methods.* (2007) 4:169-174.
[33] Scarselli, M., Li, B., Kim, S., Wess, J., *J Biol Chem.* (2007) 282:7385-7396.
[34] Baranski, T., Herzmark, P., Lichtarge, O., Gerber, B., Trueheart, J., Meng, E., Iiri, T., Sheikh, S., Bourne, H., *J Biol Chem.* (1999) 274:15757-15765.
[35] Geva, A., Lassere, T.B., Lichtarge, O., Pollitt, S.K., Baranski, T.J., *J Biol Chem* (2000) 275:35393-35401.
[36] Warne, T., Moukhametzianov, R., Baker, J.G., Nehme, R., Edwards, P.C., Leslie, A.G., Schertler, G.F., Tate, C.G., *Nature* (2011) 469:241-244.
[37] Avlani, V.A., Gregory, K.J., Morton, C.J., Parker, M.W., Sexton, P.M., Christopoulos, A., *J Biol Chem* (2007) 282:25677-25686.
[38] Massotte, D., Kieffer, B.L., *Nat Struct Mol Biol* (2005) 12:287-288.
[39] Palczewski, K., et al., *Science* (2000) 289:739-745.
[40] Xu, F., Wu, H., Katritch, V., Han, G.W., Jacobson, K.A., Gao, Z.G., Cherezov, V., Stevens, R.C., *Science* (2011).